The pH-controlled synthesis of a gold nanoparticle/polymer matrix via electrodeposition at a liquid–liquid interface

2007 J. Phys.: Condens. Matter 19 375106

(http://iopscience.iop.org/0953-8984/19/37/375106)

IOP PUBLISHING JOURNAL OF PHYSICS: CONDENSED MATTER

J. Phys.: Condens. Matter **19** (2007) 375106 (12pp) doi:10.1088/0953-8984/19/37/375106

The pH-controlled synthesis of a gold nanoparticle/polymer matrix via electrodeposition at a liquid–liquid interface

K Lepková, J Clohessy and V J Cunnane

Materials and Surface Science Institute, University of Limerick, Limerick, Republic of Ireland

E-mail: vincent.cunnane@ul.ie

Received 2 April 2007, in final form 19 June 2007
Published 13 August 2007
Online at stacks.iop.org/JPhysCM/19/375106

Abstract

A controlled synthesis of metal nanoparticles co-deposited in a polymer matrix at various pH conditions has been investigated at the interface between two immiscible phases. The pH value of the aqueous phase is modified, resulting in various types of reaction between the gold compound and the monomer. The types of electrochemical processes and their kinetic parameters are determined using both the method of Nicholson and a method based on the Butler–Volmer equation. Cyclic voltammetry is the experimental method used. A material analysis via transmission electron microscopy and particle size distribution calculations confirm that nanoparticles of different sizes can be synthesized by modification of the system pH. The stability of the generated nanocomposite is also discussed.

1. Introduction

The preparation of nanometre-sized particles has been of interest to many research groups. There have been a number of techniques for nanoparticle synthesis developed over the years using a range of metals [1–5].

Gold has been used for nanocolloid preparation and has been studied in relation to its electronic, catalytic [6] and biocompatible properties. Organometallic compounds containing the Au–P bond, such as bis(diphenylphosphines) and their bis(gold(I)) complexes, are of interest due to their anti-tumour activity [7]. And the use of gold nanoparticles in photo-thermal medicine has been described recently [8].

Because of their high surface reactivity, bare nanoparticles are unstable and tend to agglomerate [9]. Therefore, the field of synthesis of metal colloids protected with polymer represents a potential for the tailoring of new functional materials.

The attraction of gold is related to the fact that gold(I)-containing polymers often contain attractive gold–gold interactions which are known to be luminescent and can potentially be used for optical materials. $[Au(CN)_2]$-based polymers have been prepared in several cases showing

potentially useful magnetic, porous and optical properties. The vapochromic behaviour of metal–organic coordination polymers has the possibility of sensor-type applications [10, 11]. An optical screening technology for detection of genetic mutation can be based on the use of oligonucleotide–Au nanoparticle conjugates, for which gold nanoparticles are synthesized and attached to oligonucleotides via an alkyl thiol modification of the oligonucleotides [12].

Electrochemical synthesis carried out at an interface between two immiscible solutions represents a suitable method for generating metal nanocomposites, even though it has only been described in a few cases. In recent years, a liquid–liquid interface has been used to study simple electron and ion transfer between the two phases [13–17].

The first study of metal deposition at a liquid–liquid interface was published by Guainazzi *et al* [18], who reported a copper deposition at the water–1,2-dichloroethane interface. Further, the deposition of palladium and silver nanoparticles have been published [19, 20].

The electropolymerization at the liquid–liquid interface was for the first time described by Cunnane [21], when the formation of oligomers of methyl- and phenyl-pyrrole initiated by a heterogeneous electron transfer step was determined. The electrosynthesis of polymer-coated metal particles at the ITIES was described by Johans *et al* [20] introducing electrosynthesis of polyphenylpyrrole-coated silver particles at a liquid–liquid interface.

The first synthesis of gold nanoparticles in a two-phase liquid–liquid system was described by Brust *et al* [22]. In their study, the water–toluene interface was used and gold nanoparticles of 1–3 nm size were prepared by reduction of $AuCl_4^-$ ions. In another study, a successful synthesis of gold nanoparticles at the water–1,2-dichloroethane interface has also been achieved [23, 24].

Knake *et al* [25] reported a study on simultaneous nucleation of gold nanoparticles and polymerization of tyramine carried out at the water–1,2-dichloroethane interface. It was shown that when the gold ion of tetraoctylammonium tetrachloroaurate is transferred from the organic to the aqueous phase, a fast homogeneous electron transfer from the tyramine monomer reduces the gold ion. This is followed by electropolymerization and gold particle formation.

Tyramine (4-hydroxyphenylethylamine) was used as a monomer in the aqueous phase. Its usage as an immobilizer for enzymes and oligonucleotides, and for construction of biosensors, has been previously discussed in the literature [26–30].

It has been shown that electrochemistry at liquid–liquid interfaces enables the preparation of metal nanoparticles incorporated into a polymer matrix. The objective of this work is to control the fabrication of nanostructures at a water–1,2-dichloroethane interface and thereby to produce a range of nanoparticles stabilized in a polymer matrix. For this purpose, an electrochemical system consisting of the $AuCl_4^-$ ion in the organic phase and tyramine as the monomer in the aqueous phase was used.

2. Experimental details

In all aqueous solutions, ultra-pure Millipore water (18.2 MΩ), with total organic carbon content <5 ppb, was used. This was prepared using the Maxima ultra-pure water system (Elga Ltd). As an aqueous supporting electrolyte, lithium sulfate (Li_2SO_4; Fluka, >99.0%) was used. In the reference aqueous phase of the four-electrode electrochemical set-up, tetraphenylarsonium chloride (TPAsCl; Sigma Aldrich, 97%) was used. Sulfuric acid (H_2SO_4; Fluka, >95%) and sodium hydroxide (NaOH; Alfa Aesar, >97%) were used to adjust the acidic or basic environment of the aqueous phase in the pH dependence measurements. Their addition to the electrochemical system has no detrimental effect on the polarizable range.

To correct all the potentials measured by cyclic voltammetry to the Galvani scale, tetraethylammonium ion (TEACl; Fluka, >98%) was used as a standard. As a monomer for

Table 1. Chemical system for partitioning ion experiments.

Organic phase		Aqueous phase	
$TOAAuCl_4$	(x mM)	Tyramine	(y mM)
$TPAsTPBF_{20}$	(1 mM)	Li_2SO_4	(10 mM)
$LiTPBF_{20}$	(1 mM)	H_2SO_4/NaOH	

electrochemical polymerization, 4-(2-aminoethyl)-phenol (tyramine; Sigma Aldrich, 99%) was used as received in the aqueous phase. Tetraphenylarsonium tetrakis(pentafluorophenyl)borate ($TPAsTPBF_5$) was used as the organic base electrolyte.

Tetraoctylammoniumtetrachloroaurate ($TOAAuCl_4$) was used as a reagent in the organic phase. The preparation of the compounds used in the organic phase is described elsewhere [23].

All electrochemical measurements were carried out in a typical four-electrode cell [16] and analysed with an Autolab PGSTAT 100 potentiostat (Eco Chemie, Netherlands) controlled by GPES 4.9 for Windows software. In all electrochemical experiments, the half-wave potentials obtained from the cyclic voltammetry measurements were adjusted to the Galvani scale according to the formal Galvani transfer potential of the tetraethylammonium ion across the liquid–liquid interface previously reported in the literature [31].

The chemical descriptions of the electrochemical cells are given below. In these arrangements, ‖ represents a polarizable interface between the two immiscible phases.

Cell 1

$$\mathrm{Ag|AgCl|5\ mM\ TPAsCl(w)|1\ mM\ TOAAuCl_4(o) + 5\ mM\ TPAsTPBF_5(o)}$$
$$\mathrm{\|0.5\ mM\ tyramine(w) + 10\ mM\ Li_2SO_4(w)|Pt.}$$

Partitioning ion experiments were carried out in Pyrex test tubes of 20 ml volume without any external electrode system applied. An equal volume of aqueous and organic phase was used. The experimental set-up is given in table 1. Acidic and basic pH values of the aqueous phase were achieved by sulfuric acid and sodium hydroxide addition, respectively. The experimental set-up presented in this paper as a system at original pH conditions can be characterized by cell 1, and refers to an approximate value of pH 10, which is the pH value of an aqueous 1 mM solution of tyramine. The values for pK_a of tyramine as 9.74 and 10.52 are given in the literature [26]. The pH values were measured using a glass electrode (HI 8424, Hanna Instruments).

It was previously stated [25] that when the lithium ion is used as a partitioning ion in a water–1,2-dichloroethane system, the reaction between tetraoctylammonium tetrachloroaurate and tyramine proceeds resulting in formation of a nanoparticle–polymer matrix at the interface. Therefore, the lithium ion has again been used in our research to establish an interfacial Galvani potential difference of approximately 450 mV [20]. The lithium ion was introduced into the system in the form of Li_2SO_4 in the aqueous phase and $LiTPBF_{20}$ in the organic phase.

The transmission electron microscopy (TEM) images presented in this study were taken using a JEOL 2010 transmission electron microscope. The device was operated in the high-voltage mode (200 kV) and with a vacuum of approximately 1×10^{-4} Pa. A photographic camera with adjustable exposure time was part of the equipment.

The matrix generated at the liquid–liquid interface was placed on a carbon-coated grid of 3 mm in diameter (Holey 400 Cu; Agar Scientific, Ltd) and washed with ultra-pure distilled water and 1,2-dichloroethane to remove any residues of aqueous and organic base electrolytes. The images were obtained at wide range of magnitudes to describe the sample precisely.

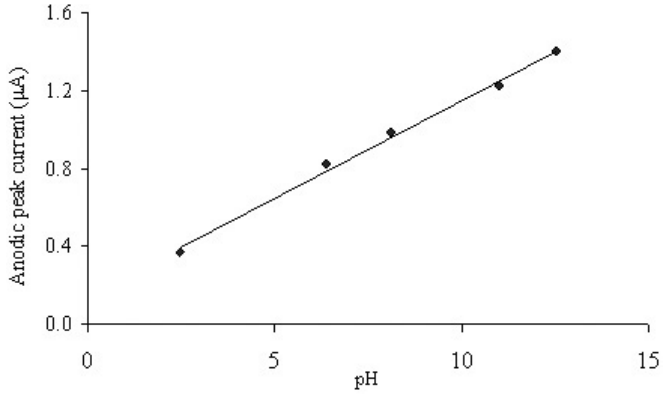

Figure 1. Forward peak current dependence on pH of the aqueous phase of the electrochemical system described in cell 1 (tyramine = 0.5 mM; $TOAAuCl_4$ = 1 mM).

3. Results and discussion

In figure 1 the values of the forward peak current representing the $AuCl_4^-$ ion transfer from the organic to the aqueous phase are plotted against the pH values of the aqueous phase. These experiments were carried out in order to determine electrochemical system behaviour when both of the reagents are present in their relevant phases and the pH value of the aqueous phase is modified. The values were recorded by cyclic voltammetry measurements using the electrochemical set-up described in cell 1, and values of the first sweep rate measured were taken. All measurements were carried out at a scan rate of 25 mV s^{-1}. The pH range of the aqueous phase varies throughout the pH range from acidic to basic values. It can be observed that the peak current density increases with increasing pH value of the aqueous phase. Thus, the pH dependence of the electrochemical process has been confirmed.

The experimental set-up described in cell 1 was used to find out whether the adjustment of the pH value of the aqueous phase can influence the transfer across the liquid–liquid interface of the reagent present in the organic phase. However, in the absence of tyramine (cell 1, tyramine = 0 mM), when the values of the forward peak current of the $AuCl_4^-$ ion transfer from the organic to the aqueous phase are plotted against the pH values of the aqueous phase, no dependence is observed. A similar result is obtained for the dependence of the half-wave potential of gold ion transfer on the pH value of the aqueous phase. The measured data are plotted in figure 2. These results show that the gold ion transfer is independent of pH changes in the aqueous phase. It also indicates that the pH modification of the aqueous phase in the two-phase system influences the structure of the monomer and potentially its reaction with the reagent in the organic phase.

The impact of system pH modification on the electrochemical reaction between the gold compound and tyramine, and on the properties of the generated matrix, was studied in detail using two electrochemical systems: a system adjusted to pH 2 and a system adjusted to pH 12.

3.1. Gold ion transfer and tyramine polymerization at pH 2

In order to see if the tyramine cation transfer across the liquid–liquid interface occurs at pH 2 of the aqueous phase, an experiment was carried without any gold compound present in the organic phase. The result is shown in figure 3. The transfer of tyramine in its protonated form occurs at the very end of the potential window and it has a half-wave Galvani scale potential

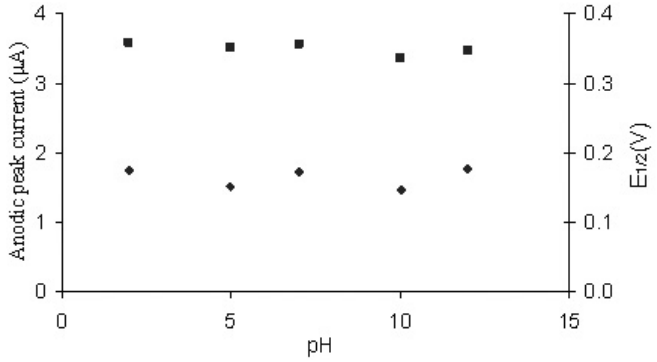

Figure 2. Forward peak current (■) and half-wave transfer potential (♦) dependence of gold ion transfer on the pH of the aqueous phase of the electrochemical system described in cell 1 (tyramine = 0 mM; $TOAAuCl_4$ = 1 mM).

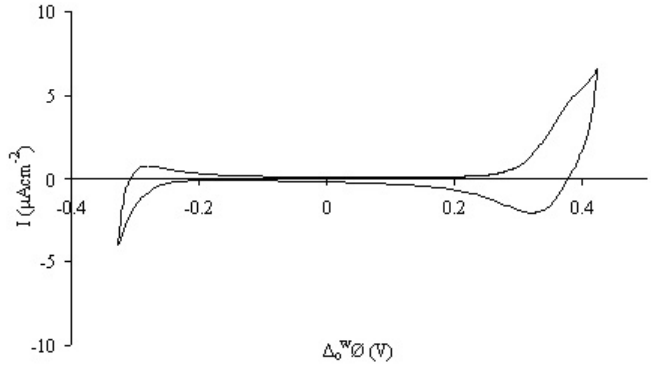

Figure 3. Cyclic voltammogram of the transfer of the tyramine cation across the interface in the absence of tetraoctylammonium tetrachloroaurate in the organic phase. The aqueous phase has been adjusted to pH 2. Cell 1.

($\Delta_o^w\phi^{1/2}$) of approximately 360 mV. The presented cyclic voltammetry response confirms that when tyramine is present at pH 2 conditions it occurs in its protonated form and carries an excess positive charge.

Figure 4 shows transfer of the $AuCl_4^-$ ion across the liquid–liquid interface when both of the reagents, tyramine and tetraoctylammonium tetrachloroaurate, are present in the system. The experiment was carried out at a range of sweep rates between 10 and 100 mV s^{-1}. According to a diagnostic test for the determination of the system type, the results obtained indicate a quasi-reversible system [33, 34]. The diffusion coefficient of the ion transfer in the organic solution is calculated using the Randles–Ševčík equation [33]. As the relation between the current obtained for the forward peak, representing the gold ion transfer across the interface, versus the square root of the measured scan rate follows the Randles–Ševčík theory, we use an equation determined for a reversible type of reaction to calculate the value of the diffusion coefficient. We also assume that the values for a quasi-reversible process lie in the transition region between reversible and irreversible processes, and the cyclic voltammetry results presented in figure 4 are closer to those theoretically obtained for a reversible reaction type. Then, the diffusion coefficient value of 1.37×10^{-8} cm^2 s^{-1} was calculated. In comparison to data previously published in the literature and to the value theoretically expected

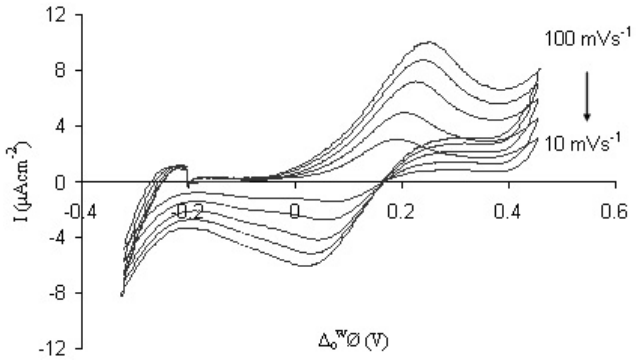

Figure 4. Cyclic voltammogram of gold ion transfer across the interface. The aqueous phase has been adjusted to pH 2. Cell 1.

for this reaction type, the value calculated from our experimental results is two orders of magnitude lower. This can be possibly explained by tyramine partitioning into the organic phase and the formation of a charged complex with the gold compound before a potential is applied to the system. This complex is further transferred to the aqueous phase after the initiation of the electrochemical process.

Using the current–potential curves measured at various sweep rates presented in figure 4, the values of peak potential differences ΔE_p ($\Delta E_p = E_p^f - E_p^r$) were calculated. E_p^f and E_p^r represent the forward and reverse peak potentials, respectively. It is theoretically stated that the current–potential curves obtained from a quasi-reversible process are a function of a dimensionless parameter ψ. Experimental values of $\Delta E_p \times n$ obtained were fitted to theoretically derived working curves of Nicholson and Shain [34, 35], showing variation of peak potential with ψ. As the diffusion coefficient and the scan rates are known, it is possible to calculate k^0 using equation (1).

$$\psi = \frac{(RT)^{1/2}k^0}{(nFD\pi v)^{1/2}}, \tag{1}$$

where ψ represents a dimensionless parameter in cyclic voltammetry, D is the diffusion coefficient ($cm^2\ s^{-1}$), v is the linear potential scan rate ($V\ s^{-1}$), n is the number of electrons, and k^0 is the standard heterogeneous rate constant ($cm\ s^{-1}$) [33–35]. The heterogeneous rate constant was estimated to be 4.52×10^{-5} $cm\ s^{-1}$. Assuming that the quasi-reversible system is usually recognized to have boundaries given in equation (2), the type of electrochemical process studied can be confirmed, as the rate constant calculated from measured data matches the region limits.

$$0.3v^{1/2} \geqslant k^0 \geqslant 2 \times 10^{-5}\ v^{1/2}\ (cm\ s^{-1}). \tag{2}$$

3.2. Gold ion transfer and tyramine polymerization at pH 12

When the pH value of the aqueous phase was adjusted to 12 and cyclic voltammetry measurements were carried out in absence of the gold ion, transfer of the tyramine cation was not observed in the potential window. This can be explained by the fact that when operating at conditions of pH 12 of the aqueous tyramine solution, tyramine does not exist as the protonated form. Even though there is no tyramine ion transfer across the liquid–liquid interface visible at the cyclic voltammetry scan, a chemical reaction between tyramine and the gold compound

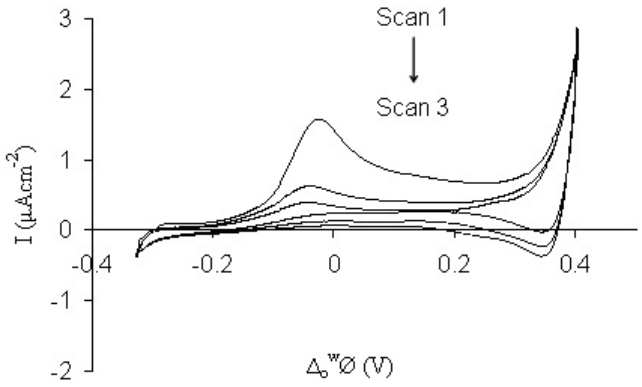

Figure 5. Cyclic voltammogram of gold ion transfer across the interface. The aqueous phase has been adjusted to pH 12. Cell 1.

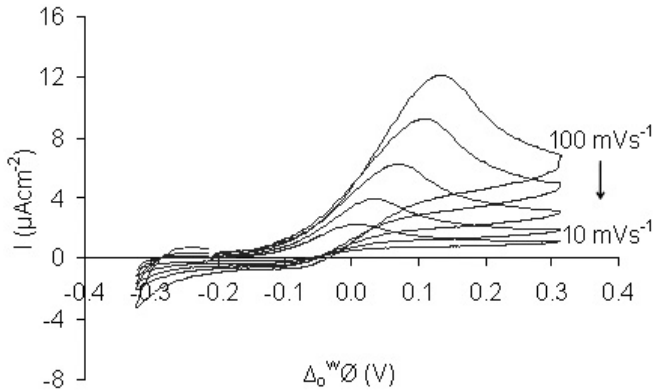

Figure 6. Cyclic voltammogram of gold ion transfer across the interface. The aqueous phase has been adjusted to pH 12. Cell 1.

still proceeds, as can be seen in figure 5, which shows the $AuCl_4^-$ ion transfer across the interface. It can be seen that the current value of the forward peak, proportionally related to the concentration of gold compound in the system, decreases with every following scan, and there is no evidence of a reverse peak. This result indicates an electrochemical–chemical (EC) reaction-type mechanism.

The $AuCl_4^-$ ion transfer across the liquid–liquid interface was again measured at various sweep rates, and the result is shown in figure 6. It can be seen that the gold ion transfer occurs at about -10 mV at the Galvani scale, which is a value different from the value obtained for the $AuCl_4^-$ ion transfer at the pH 2 conditions mentioned above, and also differs from the value published for $AuCl_4^-$ transfer in a non-modified pH electrochemical set-up (92 mV [25]).

Based on these cyclic voltammetry measurements, the electrochemical process was determined as irreversible. The main feature characterizing an irreversible system is the absence of a reverse peak, which was nearly fulfilled in our case. However, this could also be caused by a fast following reaction, and so does not fully confirm the irreversibility of a process. Therefore, system determination tests were applied and the process proved to be irreversible. The diffusion coefficient was calculated to be 6.85×10^{-5} cm^2 s^{-1} [33].

For the heterogeneous rate constant determination, a method based on Butler–Volmer equation was used, and it is mathematically described by equation (3) [35, 36]. The values of the peak potential subtracted with the standard potential ($E_p - E^0$) and I_p values were obtained from data previously shown in figure 6. The obtained values were taken with reference to an arbitrary reference potential E^0, which was taken as the standard transfer potential of the tetraethylammonium ion. By plotting experimentally known values ($E_p - E^0$) against values $\ln I_p$ determined at different scan rates, a straight line was obtained. It has a slope of $-\alpha f$ and an intercept proportional to k^0.

$$I_p = 0.227\,\mathrm{FAC}_O^* k^0 \mathrm{e}^{[-\alpha f(E_p - E^0)]} \tag{3}$$

where k^0 is the standard heterogeneous rate constant (cm s^{-1}), α is the transfer coefficient, f equals F/RT (V^{-1}), A is the area (cm^2), and C_O^* is the bulk concentration (mol cm^{-3}).

Using this method, the heterogeneous constant of the process was evaluated to be approximately 3.83×10^{-3} cm s^{-1}.

4. Nanocomposite preparation using a partitioning ion to establish Galvani potential difference

The system chemically described in table 1 was used to investigate the possibility of a metal–polymer matrix formation at the interface between two immiscible phases. For comparison, a non-modified system was also analysed.

4.1. Reagent concentration ratio dependence on chemical reaction

The effect of monomer to metal ratio in the system on the amount of matrix generated at the interface was studied using three different set-ups: (1) monomer excess in the aqueous phase (table 1, ($x = 0.2$ mM, $y = 1$ mM)), (2) tetraoctylammonium tetrachloroaurate excess in the organic phase (table 1, ($x = 1$ mM, $y = 0.5$ mM)), and (3) equal concentrations of the monomer and gold compound (table 1, ($x = 1$ mM, $y = 1$ mM)). For each of these systems, the pH range from 2 to 12 was studied. When the aqueous phase was adjusted to pH 10 and higher, the reaction was considered to be finished after 14 days when the organic phase turned from yellow to colourless, indicating that the gold compound was consumed in the reaction. The process was allowed to proceed for this period of time, and the visual results are described. When the pH of the aqueous phase was lower than 10, there was no colour change obtained in the organic phase. This can be explained by tyramine being present in its protonated form in this type of system, as was previously shown in this paper, which diminishes its ability to reduce the gold ion. As an additional supporting fact, the very slow reaction constant can be taken into account.

Similar visual results were obtained for both the experiments carried at pH lower and pH higher than 10.

When the pH of the aqueous phase was adjusted to 2 there was not enough material generated at the liquid–liquid interface for a collection for further investigation in any of the systems studied. However, the best result in terms of amount of generated material was obtained for the system in which tyramine was used in excess in the aqueous phase. In this case, there was a purple layer of approximate thickness 0.5 mm generated at the interface. Whereas, when the gold compound was used in excess in the organic phase, there was no layer visible at the interface; and only a very thin layer was generated in the system with equal reagent concentrations.

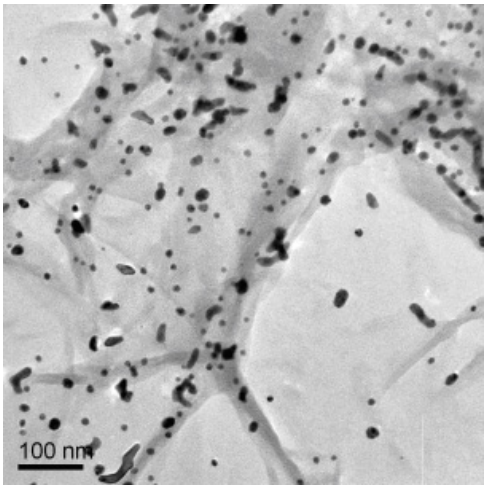

Figure 7. Transmission electron microscopy image of gold nanoparticles embedded in polytyramine matrix prepared with the aqueous phase at pH 10. Magnification: 33.5k×.

By changing the pH of the aqueous phase to 12, the generation of material at the interface was achieved in all cases studied. Similar results were obtained for experiments carried out at pH 10 conditions. There was a dark purple material of varying thickness obtained at the interface in experiments adjusted to pH 10 and a white-grey layer with visible black pieces generated in the system with aqueous phase adjusted to pH 12. When the thickness of a layer produced at the interface in these two systems was compared, the tyramine excess in the aqueous phase appeared to be the best method for gaining a sufficient amount of material for further analysis.

Based on these results, the most promising system (table 1, ($x = 0.2$ mM, $y = 1$ mM)) was used for the synthesis of nanocomposite for further analysis.

4.2. Transmission electron microscopy study of nanocomposite generated at the liquid–liquid interface

The results shown in figures 7 and 8 represent TEM images of the matrix generated at pH 10 and pH 12, respectively. The nanocomposite material was collected at the interface between the two immiscible phases after the reaction was allowed to proceed for 14 days.

For each of the samples, the TEM images were taken at various magnifications from 13.4k× up to about 268k×. Those presented in this study were recorded at 33.5k× magnification and typically describe the analysed nanomaterial. By comparison of the TEM images, one can see that a different type of material was produced by changing the pH of the aqueous phase. The particle size distribution of the gold nanoparticles was calculated by using higher-resolution images. In each case, at least 300 measurements were used for the actual calculation. Figure 9 shows the comparison of particle size distribution of these samples. It can be seen that when the nanomaterial was prepared in a pH 10 system, the majority of nanoparticles produced were bigger than 15 nm; whereas when the pH 12 conditions were applied, particles of an average size between 5 and 10 nm were obtained. This result clearly proves that by changing the pH value of the aqueous phase in the described system, it is possible to prepare gold nanoparticles of different size trapped in a polytyramine matrix.

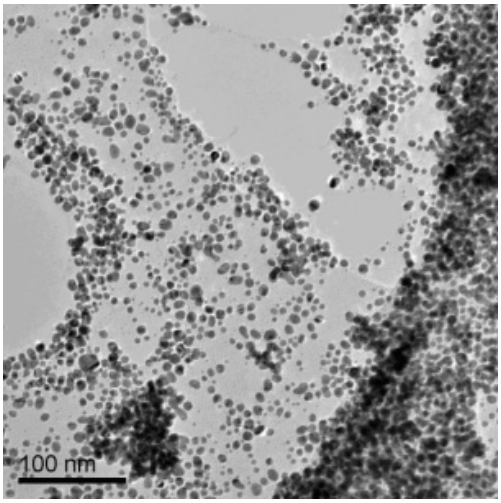

Figure 8. Transmission electron microscopy image of gold nanoparticles embedded in polytyramine matrix prepared with the aqueous phase at pH 12. Magnification: 33.5k×.

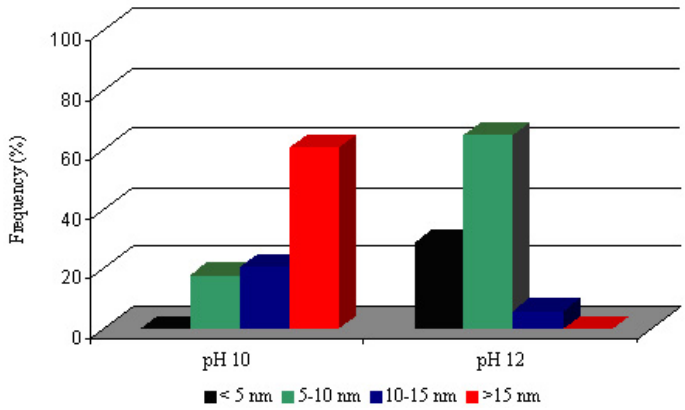

Figure 9. Particle size distribution comparison of samples generated at pH 10 and pH 12 conditions of the aqueous phase.

(This figure is in colour only in the electronic version)

Further investigation using the TEM technique was carried out in order to discover the stability of the gold nanoparticles. The TEM grids containing the samples of which images are shown in this paper were re-analysed via the TEM technique after one year. It was found that when the nanocomposite was prepared at pH 10 conditions the size of nanoparticles changed rapidly in time, since the gold particles were not stabilized enough in the polymer matrix, and an agglomeration of gold particles was obtained.

However, a different result was obtained for a sample prepared at pH 12 conditions. On repeated TEM analysis, an identical image was obtained, which confirmed the sample stability. Therefore, it can be assumed at this point that we managed to prepare a stabilized nanomaterial consisting of gold nanoparticles surrounded with polytyramine matrix. The stability of the

Table 2. Summary of kinetic parameter values of systems studied.

	pH conditions		
	pH 10	pH 2	pH 12
$AuCl_4^-$ ion transfer E (mV)	92 [25]	140	−10
Diffusion coefficient (gold ion transfer) ($cm^2\ s^{-1}$)	2.42×10^{-6} [25]	1.37×10^{-8}	6.85×10^{-5}

generated material is supported by the fact that there were no special conditions applied to store the actual TEM sample.

5. Conclusions

A preparation of gold nanoparticles surrounded in polytyramine matrix has been studied at various pH conditions between two immiscible phases. Using either sulfuric acid or sodium hydroxide, the pH value of the aqueous phase was modified throughout the pH range from 2 to 12. The impact of the pH changes of the aqueous phase system on gold ion transfer across the liquid–liquid interface is negated, whereas the pH sensitivity of tyramine, which consequently influences its chemical reaction with the gold ion, is confirmed.

Two systems, adjusted to pH 2 and to pH 12 values, were selected for a detailed description. The reaction carried out at pH 2 conditions was characterized as quasi-reversible, with a standard heterogeneous constant of 4.52×10^{-5} cm s^{-1} calculated using the method of Nicholson. An irreversible electrochemical reaction was obtained when the pH 12 conditions were established. It has a standard rate constant of 3.83×10^{-3} cm s^{-1} calculated using a method based on the Butler–Volmer equation. The values of diffusion coefficients are also given. A summary of kinetic parameter values of the studied systems is given in table 2.

The physical properties of the nanocomposite formed at the liquid–liquid interface were studied using transmission electron microscopy. For this purpose, a series of test tube reactions was carried out to obtain a sufficient amount of material at the interface. A Galvani potential difference was established using lithium ion as a partitioning ion between the two phases. The effect of reagent ratio was considered and the most promising system determined. TEM images were taken of the material generated when original and basic pH conditions were applied to the aqueous phase of the studied system. The size distribution of gold nanoparticles surrounded with polymer was calculated in each case. It was shown that nanoparticles of an average size greater than 15 nm were obtained at pH 10 conditions, whereas particles of size between 5 and 10 nm were formed when pH 12 conditions were applied to the system. These results clearly prove that by pH modification of the aqueous phase of the studied system, nanoparticles of different size can be synthesized. The stability of gold nanoparticles prepared at basic pH conditions was confirmed by re-analysing the sample after a certain period of time, when an identical image was obtained.

Acknowledgments

The authors thank Professor Shohei Nakahara and Dr David A Tanner for their help in the acquisition of transmission electron microscopy images. Their advice is greatly appreciated. We also thank the European Commission for funding the SUSANA Research and Training Network (Supramolecular Self-Assembly of Interfacial Nanostructures), Project No. HPRN-CT-2002-00185.

References

[1] Pileni M P 1997 *Langmuir* **13** 3266
[2] Bandyopadhyay S and Chakravorty D J 1997 *Mater. Res.* **12** 2719
[3] Devenish R W, Goulding T, Heaton B T and Whyman R 1996 *J. Chem. Soc. Dalton Trans.* **5** 673
[4] Kumar R V, Diamant Y and Gedanken A 2000 *Chem. Mater.* **12** 2301
[5] Yin Y, Xu X, Ge X, Xia C and Zhang Z 1998 *Chem. Commun.* 1641
[6] Toshima N, Harada M, Yamazaki Y and Asakura K 1992 *J. Phys. Chem.* **96** 9927–33
[7] Mirabelli C K, Jensen B D, Mattern M R, Sung C M, Mong S M, Hill D T, Dean S W, Schein P S, Johnson R K and Crooke S T 1986 *Anti-Cancer Drug Des.* **1** 223–34
[8] Pissuwan D, Valenzuela S M and Cortie M B 2006 *Trends Biotechnol.* **24** 62–7
[9] Manna A, Chen P L, Akiyama H, Wei T-X, Tamada K and Knoll W 2003 *Chem. Mater.* **15** 20–8
[10] Katz M J, Aguiar P M, Batchelor R J, Bokov A A, Ye Z G, Kroeker S and Leznoff D B 2006 *J. Am. Chem. Soc.* **128** 3669–76
[11] Lefebvre J, Batchelor R J and Leznoff D B 2004 *J. Am. Chem. Soc.* **126** 16117–25
[12] Redmond G 2006 *Gold 2006: Conf. Abstract Booklet* p 82
[13] Geblewicz G and Schiffrin D J 1988 *J. Electroanal. Chem.* **244** 27–37
[14] Cunnane V J, Geblewicz G and Schiffrin D J 1995 *Electrochim. Acta* **40** 3005–14
[15] Cunnane V J, Schiffrin D J, Beltran C, Geblewicz G and Solomon T 1998 *J. Electroanal. Chem.* **247** 203–14
[16] Samec Z, Mareček V, Koryta J and Khalil M W 1977 *J. Electroanal. Chem.* **83** 393–7
[17] Cheng Y and Schiffrin D J 1991 *J. Eletroanal. Chem.* **314** 153–63
[18] Guainazzi M, Silvestri G and Suravalle G 1975 *J. Chem. Soc. Chem. Commun.* 200
[19] Johans C, Lahtinen R, Kontturi K and Schiffrin D J 2000 *J. Electroanal. Chem.* **488** 99–109
[20] Johans C, Clohessy J, Fantini S, Kontturi K and Cunnane V J 2002 *Electrochem. Commun.* **4** 227–30
[21] Cunnane V J and Evans U 1998 *Chem. Commun.* **19** 2163–4
[22] Brust M, Walker M, Bethell D, Schiffrin D J and Whyman R 1994 *J. Chem. Soc. Chem. Commun.* 801
[23] Cheng Y and Schiffrin D J 1996 *J. Chem. Soc. Faraday Trans.* **92** 3865–71
[24] Su B, Abid J P, Fermin D J, Girault H H, Hoffmannová H, Krtil P and Samec Z 2004 *J. Am. Chem. Soc.* **126** 915–9
[25] Knake R, Fahmi A W, Tofail S A M, Clohessy J, Mihov M and Cunnane V J 2005 *Langmuir* **21** 1001–8
[26] Tran L D, Piro B, Pham M C, Ledoan T, Angiari C, Dao L H and Teston F 2003 *Synth. Met.* **139** 251–62
[27] Situmorang M, Gooding J J, Hibbert D B and Barnett D 2002 *Electroanalysis* **14** 17
[28] Situmorang M, Gooding J J, Hibbert D B and Barnett D 2001 *Electroanalysis* **13** 1469
[29] Situmorang M, Gooding J J, Hibbert D B and Barnett D 1999 *Anal. Chim. Acta* **394** 211
[30] Palmisano F, DeBenedetto G E and Zambonin C G 1997 *Analyst* **122** 365
[31] Wandlowski T, Mareček V and Samec Z 1990 *Electrochim. Acta* **35** 1173–5
[32] Greef R, Peat R, Peter L M, Pletcher D and Robinson J 1990 *Instrumental Methods in Electrochemistry* 2nd edn (Great Britain: Ellis Horwood Limited)
[33] Bard A J 2001 *Electrochemical Methods: Fundamentals and Applications* 2nd edn (New York: Wiley)
[34] Nicholson R S 1965 *Anal. Chem.* **37** 1351–5
[35] Nicholson R S and Shain I 1964 *Anal. Chem.* **36** 706–23
[36] Aoki K 2005 *Electrochem. Commun.* **7** 523–7